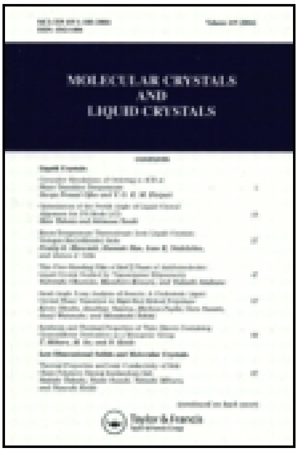

Molecular Crystals and Liquid Crystals
Publication details, including instructions for authors and subscription information:
http://www.tandfonline.com/loi/gmcl20

Synthesis and Photovoltaic Performance of Long Wavelength Absorbing Organic Dyes for Dye-Sensitized Solar Cells

Sang Ah Kim [a], Hyo Jeong Jo [a], Mi Ran Jung [a], Young Cheol Choi [b], Do Kyung Lee [b], Moonyong Lee [a] & Jae Hong Kim [a]

[a] School of Display and Chemical Engineering, Yeungnam University, Gyeongsan, Gyeongsangbuk-do, 712-749, Republic of Korea

[b] R&D Affairs Department, Gumi Electronics and Information Technology Research Institute, Gumi, Gyeongsangbuk-do, 730-853, Republic of Korea

To cite this article: Sang Ah Kim, Hyo Jeong Jo, Mi Ran Jung, Young Cheol Choi, Do Kyung Lee, Moonyong Lee & Jae Hong Kim (2011): Synthesis and Photovoltaic Performance of Long Wavelength Absorbing Organic Dyes for Dye-Sensitized Solar Cells, Molecular Crystals and Liquid Crystals, 551:1, 283-294

To link to this article: http://dx.doi.org/10.1080/15421406.2011.601189

Mol. Cryst. Liq. Cryst., Vol. 551: pp. 283–294, 2011
Copyright © Taylor & Francis Group, LLC
ISSN: 1542-1406 print/1563-5287 online
DOI: 10.1080/15421406.2011.601189

Synthesis and Photovoltaic Performance of Long Wavelength Absorbing Organic Dyes for Dye-Sensitized Solar Cells

SANG AH KIM,[1] HYO JEONG JO,[1] MI RAN JUNG,[1]
YOUNG CHEOL CHOI,[2] DO KYUNG LEE,[2,*]
MOONYONG LEE,[1] AND JAE HONG KIM[1,*]

[1]School of Display and Chemical Engineering, Yeungnam University,
Gyeongsan, Gyeongsangbuk-do 712-749, Republic of Korea
[2]R&D Affairs Department, Gumi Electronics and Information Technology
Research Institute, Gumi, Gyeongsangbuk-do 730-853, Republic of Korea

We prepared novel organic photo-sensitizers based on a carbazole framework containing various acceptors with thiophene bridge units in the chromophore for the application to dye-sensitized solar cell (DSSC). Furthermore, organic dyes without bridge in the chromophore also synthesized to investigate the correlation between conjugation lengths and photon-to-current efficiency (PCE). Compared to non-bridged dyes, the DSSCs device containing multi-anchoring dyes with thiophene bridge exhibited much higher PCEs, resulting from efficient electron extraction pathways, higher molar extinction coefficients, and better light absorption in longer wavelengths.

Keywords Dye-sensitized solar cells; Organic Photosensitizers; Multi-anchoring dyes; Carbazole chromophore; Photovoltaic performances

Introduction

The supply of renewable energy sources has been considered as the most significant research field for human life during the last years. One of promising candidates for them is the solar energy, since it is renewable, clean, and inexhaustible resource. The improvement of solar energy-to-electricity conversion efficiency has continued to be an important research area of dye-sensitized solar cell (DSSC).

A typical DSSC is constructed with dye-absorbed wide band gap oxide semiconductor electrode such as TiO_2 or ZnO, electrolyte containing I^-/I_3^- redox couples, and Pt-coated counter electrode [1–7]. The photo-sensitizing dye plays the important roles in capturing the photons and generating the electron-hole pair, as well as transferring them to the interface of the semiconductor.

Organic dye molecules have been employed recently as promising candidates for the photo-sensitizer in DSSC, because of their great potential advantages (high molar extinction coefficient, convenient, and customized molecular design) for the photophysical

---

[*] Corresponding authors. E-mail: dklee@geri.re.kr, jaehkim@ynu.ac.kr

and photochemical properties and low-cost production [8–16]. Usually, organic dyes have an intra-molecular donor-acceptor structure called as the push-pull architecture. Upon light irradiation, intra-molecular charge transfer from the electron donor to the electron acceptor is induced and a subsequent electron transfer to TiO_2 wide band gap semi-conductors via the anchoring group takes place.

We had reported that the organic dyes with double electron acceptors exhibited the high power conversion efficiency in the DSSC due to the increase of electron extraction paths from electron donor as compared with that of single electron acceptor type [10]. Also, this earlier report had the important implications for the needs of further studies on the organic dyes containing multi-acceptors with a viewpoint of photovoltaic performance.

In this work, we have studied on the synthesis and characterization of the organic dyes containing different kinds of electron acceptor moieties in a molecule. In particular, photovoltaic properties for the DSSC devices are mainly discussed.

Experimental

Synthesis

Materials. All commercially available starting materials and solvents were purchased from Aldrich, TCI, and ACROS Co. and used without further purification unless otherwise stated. HPLC grade toluene and tetrahydrofuran (THF) were purchased from Samchun chemical and distilled from CaH_2 immediately before use.

10-hexyl-10H-carbazole (1)

An oven dried 250 ml round bottom flask was charged with 100 ml DMF, 1-bromohexane (11.8 g, 0.071 mol) and sodium hydride (1.72 g, 0.071 mol). Then, DMF solution of carbazole (10 g, 0.059 mol) was added into the mother solution and the reaction mixture was kept for 6 h at room temperature. After completion of the reaction, the solution was neutralized with dilute HCl aqueous solution. The mixture was extracted with chloroform/water. The dried solution was concentrated. The resulting crude oily product was purified by silica gel column chromatography (only hexane). Yield: 5.4 g (82%). ^{1}H NMR (300 MHz, $CDCl_3$): δ 8.14(d, J = 7.5 Hz, 2H), 7.59(d, J = 8.1 Hz, 2H), 7.43(t, J = 7.3 Hz, 2H), 7.19(t, J = 7.3 Hz, 2H), 4.38(t, J = 7.1 Hz, 2H), 1.76-0.80(m, 11H)

3,6-dibromo-9-hexyl-9H-carbazole (2)

Bromine (2 ml, 0.035 mol) was slowly added using a syringe to the solution of 10-hexyl-10H-carbazole (4.0 g, 0.016 mol) in 40 mL of dichloromethane. After stirring the mixture at room temperature for 12 h, the reaction was terminated by adding dilute aqueous sodium hydroxide (0.1 M). The reaction mixture was extracted using dichloromethane and water. The organic layer was separated and dried over anhydrous magnesium sulfate. The crude product was purified using column chromatography with hexane as the eluent. The product was colorless solid. Yield: 5.4 g (82%). ^{1}H NMR (300 MHz, $CDCl_3$): δ 8.05(d, J = 1.8 Hz, 2H), 7.48(dd, J_1 = 8.1 Hz, J_2 = 1.8H, 2H), 7.20(d, J = 8.1 Hz, 2H), 4.18(t, J = 7.1 Hz, 2H), $1.84 - 0.83$(m, 11H).

9-hexyl-3,6-di(thiophen-2-yl)-9H-carbazole (3)

An oven dried 250 ml round bottom flask was charged with 100 ml dry THF (50 ml), 3,6-dibromo-9-hexyl-9H-carbazole (5 g, 0.012 mol). The solution was tributyl(thiophen-2-yl)stannane (10.48 ml, 0.033 mol). Then, $Pd(PPh_3)_4$ (0.43 g, 0.61 mmol) was added into the mother solution and the reaction mixture was kept for 10 h at room temperature. The mixture was stirred at 65°C for overnight under nitrogen atmosphere. After THF was removed under vacuum, the reaction mixture was poured into water and extracted with dichloromethane and water. The solvent was removed, and the product was purified using column chromatography on a silica gel with dichloromethane/hexane (volume ratio 1:3). The product was obtained as yellow solid. Yield: 3.5 g (69%). ^{1}H NMR (300 MHz, $CDCl_3$): δ 8.35(d, J = 1.5 Hz, 2H), 7.75(dd, J_1 = 8.4 Hz, J_2 = 1.5 2H), 7.40(d, J = 8.4 Hz, 2H), 7.37(d, J = 3.3 Hz, 2H), 7.28(d, J = 3.4 Hz, 2H), 7.12(t, J = 3.4 Hz, 2H), 4.31(t, J = 7.2 Hz, 2H), 1.91−0.84(m, 11H).

5,5′-(9-hexyl-9H-carbazole-3,6-diyl)dithiophene-2-carbaldehyde (4)

9-Hexyl-3,6-di(thiophen-2-yl)-9H-carbazole (2.5 g, 6 mmol) was dissolved in 1,2-dichloroethane and DMF (1.16 ml, 0.015 mol), and (1.4 ml, 0.015 mol) of phosphorus oxychloride was carefully added through a dropping funnel, keeping the reaction temperature below 0°C. After the complete addition of $POCl_3$, the reaction solution had a red color and was stirred for 8 h at reflux. Then the mixture was poured into water. The solution was neutralized with a sodium hydroxide solution and extracted with dichloromethane. The formed precipitate was filtered off, dried over $MgSO_4$, and purified using column chromatography on a silica gel with hexane/dichloromethane (volume ratio 1:9). The product was obtained as a yellow powder. Yield: 2.2 g (77%). ^{1}H NMR (300 MHz, $CDCl_3$): δ 9.95(s, 2H), 8.43(s, 2H), 7.82(d, J = 8.4 Hz, 2H), 7.79(d, J = 3.9 Hz, 2H), 7.49(d, J = 3.9 Hz, 2H), 7.46(d, J = 8.7 Hz, 2H), 4.33(t, J = 7.2 Hz, 2H), 1.92–0.84 (m, 11H).

3,3′-(5,5′-(9-hexyl-9H-carbazole-3,6-diyl)bis(thiophene-5,2-diyl))bis(2-cyanoacrylic acid) (LOFM1)

In a dried 100 ml, round bottom flask, 5,5′-(9-hexyl-9H-carbazole-3,6-diyl)dithiophene-2-carbaldehyde (0.5 g, 1.06 mmol), cyano acetic acid (0.225 g, 2.65 mmol) ammonium acetate (0.204 g, 2.65 mmol) were dissolved in Acetic acid (20 ml). After heating the solution at 110°C for 12 h, the solvent was evaporated to obtain a dark solid. It was poured into 100 ml of water, and solution was extracted with chloroform. The resulting product was purified by silica gel column chromatography chloroform/Methanol (volume ratio 9:1). Yield: 0.5 g (77%). ^{1}H NMR (300 MHz, DMSO): δ 8.81(s, 2H), 8.47(s, 2H), 8.04(d, J = 3.6 Hz, 2H), 7.93(d, J = 7.5 Hz, 2H), 7.84(d, J = 3.9 Hz, 2H), 7.77(d, J = 8.4 Hz, 2H), 4.45 (t, J = 7.2 Hz, 2H), 1.91−0.81 (m, 11H).

3,3′-(5,5′-(9-hexyl-9H-carbazole-3,6-diyl)bis(thiophene-5,2-diyl))bis(2-cyanoacrylic acid) (LOFM2)

In a dried 100 ml, round bottom flask, 5,5′-(9-hexyl-9H-carbazole-3,6-diyl)dithiophene-2-carbaldehyde (0.3 g, 0.636 mmol), rhodanine acetic acid (0.2 g, 1.59 mmol) ammonium acetate (0.122 g, 1.59 mmol) were dissolved in Acetic acid (40 ml) under argon. After heating the solution at 110°C for 7 h, the solvent was evaporated to obtain a dark solid. The resulting product was purified by silica gel column chromatography Ethyl Acetate

/Methanol (volume ratio 9:1). Yield: 0.45 g (86%). ^{1}H NMR (300 MHz, DMSO): δ 8.79(s, 2H), 8.13(s, 2H), 7.93(d, J = 9 Hz, 2H), 7.83(m, 4H), 7.70(d, J = 8.4 Hz, 2H), 4.69(s, 4H), 4.41(t, J = 7.2 Hz, 2H), 1.72−1.25(m, 11H).

4,4′-(5,5′-(9-hexyl-9H-carbazole-3,6-diyl)bis(thiophene-5,2-diyl))bis(methan-1-yl-1-ylidene)bis(5-oxo-1-phenyl-4,5-dihydro-1H-pyrazole-3-carboxylic acid) (LOFM3)

In a dried 100 ml, round bottom flask, 5,5′-(9-hexyl-9H-carbazole-3,6-diyl)dithiophene-2-carbaldehyde (0.2 g, 0.42 mmol), 5-oxo-1-phenyl-4,5-dihydro-1H-pyrazole-3-carboxylic acid (0.21 g, 1.06 mmol) ammonium acetate (0.081 g, 1.06 mmol) were dissolved in Acetic acid (40 ml) under argon. After heating the solution at 110°C for 4 h, the solvent was evaporated to obtain a dark solid. The resulting product was purified by silica gel column chromatography Ethyl Acetate/Methanol (volume ratio 8:2). Yield: 0.28 g (80%). ^{1}H NMR (300 MHz, DMSO): δ 8.93(s, 2H), 8.84(s, 2H), 8.33(d, J = 3.9 Hz, 2H), 8.04(d, J = 7.2 Hz, 2H), 7.97(m, 4H), 7.88(d, J = 3.5 Hz, 2H), 7.79(d, J = 8.4 Hz, 2H), 7.49(t, J = 7.8 Hz, 4H), 7.28(t, J = 7.5 Hz, 2H), 4.47(t, J = 7.2 Hz, 2H), 1.82−0.80 (m, 11H).

9-hexyl-9H-carbazole-3,6-dicarbaldehyde (5)

10-Hexyl-10H-carbazole (5.05 g, 0.02 mol) was dissolved in 1,2-dichloroethane and DMF (3.42 ml, 0.05 mol), and (7.6 g, 0.05 mol) of phosphorus oxychloride was carefully added through a dropping funnel, keeping the reaction temperature below 0°C. After the complete addition of $POCl_3$, the reaction solution had a red color and was stirred for 14 h at reflux. Then the mixture was poured into water. The solution was neutralized with a sodium hydroxide solution and extracted with dichloromethane. The formed precipitate was filtered off, dried over $MgSO_4$, and purified using column chromatography on a silica gel with Hexane/Ethyl Acetate (volume ratio 4:1). The product was obtained as a white powder. Yield: 4 g (65%). ^{1}H NMR (300 MHz, $CDCl_3$): δ 10.14(s, 2H), 8.68(s, 2H), 8.10(d, J = 8.7 Hz, 2H), 7.56(d, J = 8.7 Hz, 2H), 4.40(t, J = 7.2 Hz, 2H), 1.94–0.84 (m, 11H).

3,3′-(9-hexyl-9H-carbazole-3,6-diyl)bis(2-cyanoacrylic acid) (LOFM4)

In a dried 100 ml, round bottom flask, 9-hexyl-9H-carbazole-3,6-dicarbaldehyde (0.15 g, 0.48 mmol), cyano acetic acid (0.108 g, 0.63 mmol) ammonium acetate (0.054 g, 0.63 mmol) were dissolved in Acetic acid (20 ml). After heating the solution at 110°C for 12 h, the solvent was evaporated to obtain a yellow solid. It was poured in to 100 ml of water, and solution was extracted with chloroform. The resulting product was purified by silica gel column chromatography Chloroform. Yield: 0.18 g (83%). ^{1}H NMR (300 MHz, DMSO): δ 8.88(s, 2H), 8.52(s, 2H), 8.34(d, J = 8.7 Hz, 2H), 7.95(d, J = 8.7 Hz, 2H), 4.51(t, J = 7.2 Hz, 2H), 1.80–0.80(m, 11H).

2,2′-(5Z,5′Z)-5,5′-(9-hexyl-9H-carbazole-3,6-diyl)bis(methan-1-yl-1-ylidene) bis(4-oxo-2-thioxothiazolidin-3-yl-5-ylidene)diacetic acid (LOFM5)

In a dried 100 ml, round bottom flask, 9-hexyl-9H-carbazole-3,6-dicarbaldehyde (0.15 g, 0.48 mmol), rhodanine acetic acid (0.12 g, 0.63 mmol) ammonium acetate (0.054 g, 0.63 mmol) were dissolved in Acetic acid (30 ml). After heating the solution at 110°C for 10 h, the solvent was evaporated to obtain a orange solid. The resulting product was purified by silica gel column chromatography Chloroform. Yield: 0.25 g (78%). ^{1}H NMR (300 MHz, DMSO): δ 8.62(s, 2H), 8.08(s, 2H), 7.89(d, J = 8.7 Hz, 2H), 7.81(d, J = 8.7 Hz, 2H), 4.77(s, 4H), 4.48(t, J = 7.2 Hz, 2H), 1.80–0.78(m, 11H).

4,4′-(9-hexyl-9H-carbazole-3,6-diyl)bis(methan-1-yl-1-ylidene)bis(5-oxo-1-phenyl-4,5-dihydro-1H-pyrazole-3-carboxylic acid) (LOFM6)

In a dried 100 ml, round bottom flask, 9-hexyl-9H-carbazole-3,6-dicarbaldehyde (0.15 g, 0.48 mmol), 5-oxo-1-phenyl-4,5-dihydro-1H-pyrazole-3-carboxylic acid (0.13 g, 0.63 mmol) ammonium acetate (0.054 g, 0.63 mmol) were dissolved in Acetic acid (40 ml). After heating the solution at 110°C for 15 h, the solvent was evaporated to obtain a red solid. The resulting product was purified by silica gel column chromatography Chloroform. Yield: 0.25 g (75%). ^{1}H NMR (300 MHz, DMSO): δ 9.49(s, 2H), 8.99(d, J = 9.0 Hz, 2H), 8.89(s, 2H), 7.95(d, J = 7.5 Hz, 4H), 7.89(d, J = 9.0 Hz, 2H), 7.50(t, J = 7.9 Hz, 4H), 7.31(t, J = 7.3 Hz, 2H), 4.52(t, J = 7.2 Hz, 2H), 1.83−0.79(m, 11H).

Instrumental Analysis

^{1}H NMR spectra were recorded on Bruker Advance NMR 300 Hz spectrometer using $CDCl_3$ and DMSO-d_6 purchased from Cambridge Isotope Laboratories, Inc. The redox properties of six dyes were examined using cyclic voltammetry (Model:CV-BAS-Epsilon). The electrolyte solution employed was 0.10 M tetrabutylammonium hexafluorophosphate ($TBAPF_6$) in freshly dried acetonitrile. The Ag/AgCl and Pt wire (0.5 mm in diameter) electrodes were utilized as reference and counter electrodes, respectively. The scan rate was fixed at 100 mV/s.

Assembly and Characterization of DSSCs

The conducting glass substrate (FTO; TEC8, Pilkington, 8 Ω/cm^2, Thickness of 2.3 mm) was cleaned in ethanol by ultrasonication. TiO_2 pastes were prepared using ethyl cellulose (Aldrich), Lauric acid (Fluka) and Terpineol (Aldrich). The size of TiO_2 particles is ca. 20–30 nm. The prepared TiO_2 paste was coated on the pre-cleaned glass substrate using doctor-blade, and sintered at 500°C for 30 min. The thickness of the sintered TiO_2 layer was measured with Alpha-step IQ surface profiler (KLA Tencor). The other TiO_2 paste was re-coated over the sintered layer using ca. 250 nm size of TiO_2 particle as a scattering layer, and then sintered again at 500°C for 30 min. The prepared TiO_2 film was dipped in 0.04 M of $TiCl_4$ aqueous solution at 70°C for 30 min. For dye adsorption, the annealed TiO_2 electrodes were immersed in dye solution (0.5 mM of dye in DMF; Triphenylamine series, N3/N719) at 50°C for 3 hours. Pt counter electrodes were prepared by thermal reduction of thin film formed from 7 mM of H_2PtCl_6 in 2-propanol at 400°C for 20 min. The dye-adsorbed TiO_2 electrode and Pt counter electrode were assembled using 60 μm-thick Surlyn (Dupont 1702) as a bonding agent. A liquid electrolyte was introduced through a pre-punctured hole on the counter electrode. The electrolyte was composed of 3-propyl-1-methyl-imidazolium iodide (PMII, 0.7 M), lithium iodide (LiI, 0.2 M), iodine (I_2, 0.05 M), *t*-butylpyridine (TBP, 0.5 M) in acetonitrile/valeronitrile (85:15). The active areas of dye-adsorbed TiO_2 films were estimated by a digital microscope camera with an image-analysis-software (Moticam 1000).

Results and Discussion

Synthesis and Electo-optical Properties of Organic Dyes

The intra-molecular electron donor-acceptor type of organic dyes, which are containing carbazole as an electron donor with various acceptor moieties and thiophene bridge units in the chromophore, were designed to investigate the correlations with the kinds of acceptors, conjugation lengths and photon-to-current efficiency, as shown in Scheme 1. We synthesized intermediates with mono- and bis-aldehyde containing thiophene bridges, which were separated successively by using the column chromatography. The organic photo-sensitizers containing multi-electron acceptor with various anchoring groups and thiophene bridge units, LOFM1 ~ LOFM3, and without thiophene bridge LOFM4 ~ LOFM6 were synthesized successfully.

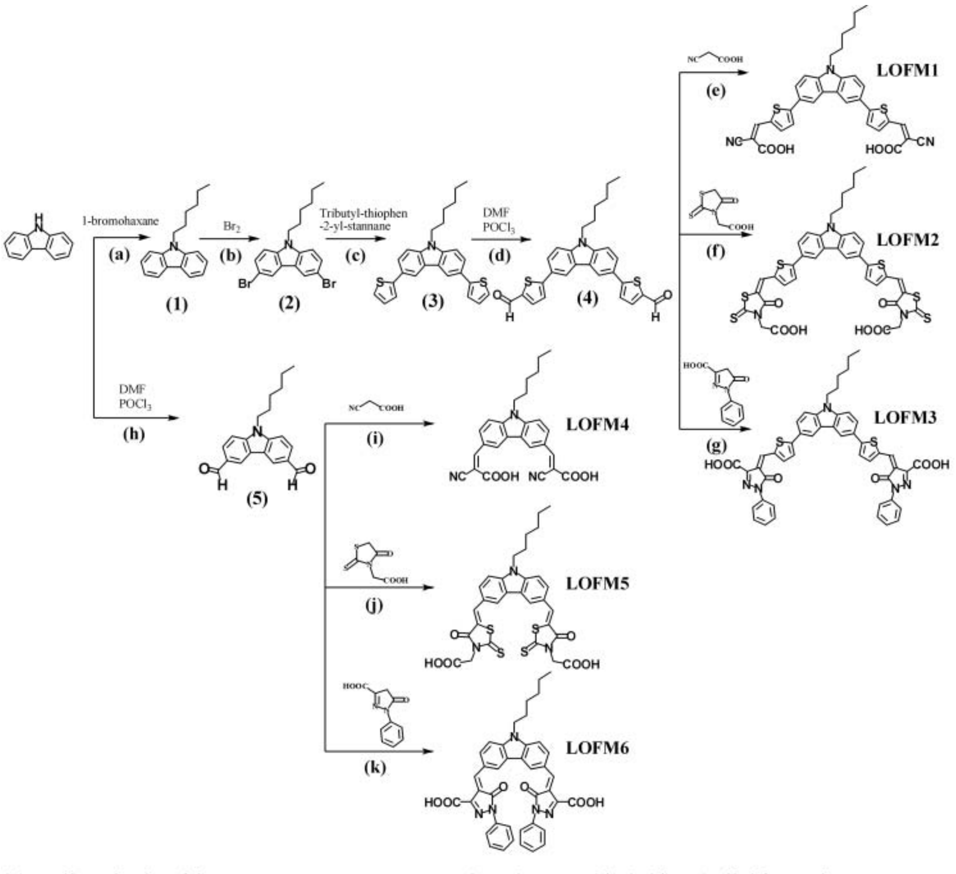

(a) sodium hydroxide, DMF (b) CH_2Cl_2 (c) $PdCl_2(PPh_3)_2$, THF(dry) (d) 1,2-dichloroethane
(e) NH_4OAc, glacial acetic acid (f) NH_4OAc, glacial acetic acid (g) NH_4OAc, glacial acetic acid
(h) 1,2-dichloroethane (i) NH_4OAc, glacial acetic acid (j) NH_4OAc, glacial acetic acid
(k) NH_4OAc, glacial acetic acid.

Scheme 1. Synthesis of organic dyes.

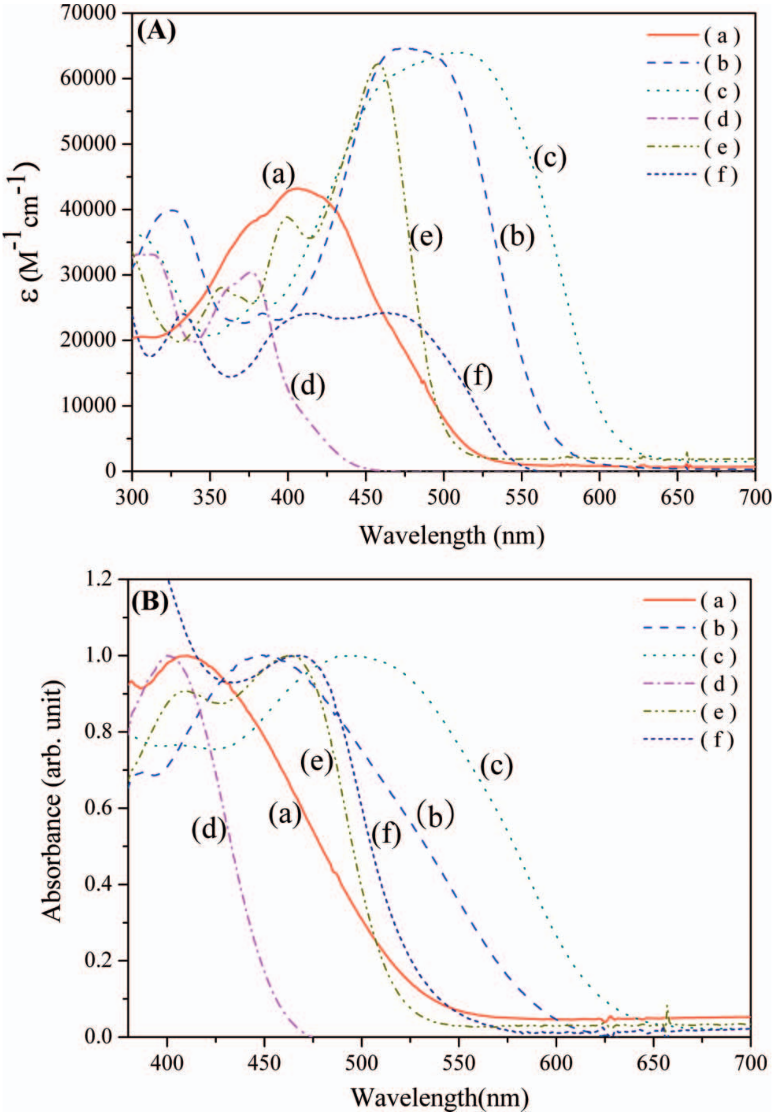

Figure 1. (A) Absorption spectra of the organic dyes in the DMF solution. (a = LOFM1, b = LOFM2, c = LOFM3, d = LOFM4, e = LOFM5, f = LOFM6) (B) Normalized absorption spectra of the organic dyes that were adsorbed onto the TiO_2 films. (a = LOFM1, b = LOFM2, c = LOFM3, d = LOFM4, e = LOFM5, f = LOFM6).

Figure 1 shows the UV-Vis absorption spectra of the synthesized dyes in DMF solution (a) and on the TiO_2 film state (b). The optical and electrochemical properties of the organic dyes are summarized in Table 1. The maximum absorption wavelength (λ_{max}) of the organic dye corresponding to the π–π^* transitions in the conjugated molecules appeared from 400 nm to 507 nm with molar extinction coefficient (ε_{max}) of 2.4×10^4 M^{-1} cm^{-1} to 6.4×10^4 M^{-1} cm^{-1}, as seen in Table 1. The organic dyes with strong electron acceptor moieties in a chromophore, LOFM3 and LOFM6, exhibited strong bathochromic shift in the λ_{max},

Table 1. Electrochemical parameters of the organic dyes.

Dye	ε_{max}[a] /M^{-1} cm^{-1}	λ_{max} nm Soln.	TiO_2[b]	$E_{0–0}$ (eV)[c] (abs)	E_{ox}[d] (V vs NHE)	E_{ox}–$E_{0–0}$[e] (V vs NHE)	HOMO (eV)	LUMO (eV)
LOFM1	43243	406	411	2.403	1.324	−1.079	−5.718	−3.315
LOFM2	64658	474	454	2.183	1.268	−0.915	−5.662	−3.479
LOFM3	64009	507	493	2.033	1.296	−0.737	−5.690	−3.657
LOFM4	30580	389	400	3.024	1.533	−1.491	−5.929	−2.905
LOFM5	62309	458	462	2.489	1.474	−1.015	−5.870	−3.381
LOFM6	23569	464	468	2.275	1.440	−0.835	−5.830	−3.555

[a]Maximum absorption and extinction coefficient at the maximum absorption of the dyes in the DMF solution. [b]Maximum absorption of the dyes that were adsorbed onto the TiO_2 films. [c]$E_{0–0}$ (band gap) was determined from the intersection of the absorption and emission spectra in the DMF solution. [d]The oxidation potential (E_{HOMO}) of the dye was measured using the cyclic voltammogram in the DMF solution. [e]$E_{ox} - E_{0–0} = E_{LUMO}$.

compared to LOFM1 and LOFM4, due to the low LUMO values. It should be noted that the λ_{max} and ε_{max} of organic dyes containing thiophene bridge units are enhanced, owing to its longer conjugated π-chromophore, which can improve the light harvesting efficiency (or photogenerated electron-hole pairs) of organic dye. The blue-shift of absorption peak may be caused by the formation of the H-aggregate of organic dyes on the TiO_2 surface [17].

To ensure regeneration of the dye molecules, the highest occupied molecular orbital (HOMO) level of the dye molecules should be more positive than the redox potential of I_3^-/I^- in the electrolyte, and the energy of the lowest unoccupied molecular orbital (LUMO) must be more negative than that of the conduction band edge in TiO_2. The HOMO and LUMO energy levels of the dye molecules were estimated by cyclic voltammetry, as shown in Table 1.

Photovoltaic Performances of the DSSCs with Organic Dyes

Figure 2 shows photocurrent-voltage (I–V) curves (A) and the incident photon-to-current efficiency (IPCE) spectra (B) of the DSSCs containing different organic dyes under illumination of simulated solar light (AM 1.5, 100 mW/cm^2). The corresponding results are indicated in Table 2. The higher efficiencies were achieved in the DSSC with LOFM1 ~ LOFM3 rather than LOFM4 ~ LOFM6, mainly owing to the higher short-circuit current (J_{sc}) value (see Table 2). This is originated in their improved light harvesting efficiency, which is resulted from the longer conjugated π-chromophore. Among the organic dyes, LOFM1 containing bis-anchors/acceptors in carbazole chromophore with thiophene bridge unit exhibited highest energy conversion efficiency, which is 3.0%, as revealed in Table 2. The IPCEs of DSSCs with organic dyes were also measured, and the result is represented in Figure 2(B). The integrated IPCE values were consistent with the J_{sc} values of organic dyes.

The DSSCs with the LOFM1 ~ LOFM3 exhibited slightly lower open-circuit voltage (V_{oc}) than those with LOFM4 ~ LOFM6. The properties of charge transport in DSSCs have been evaluated by measuring their impedance spectra (IS) under light illumination condition. Under illumination, a DSSC is biased by the photovoltage, and thus photocurrent

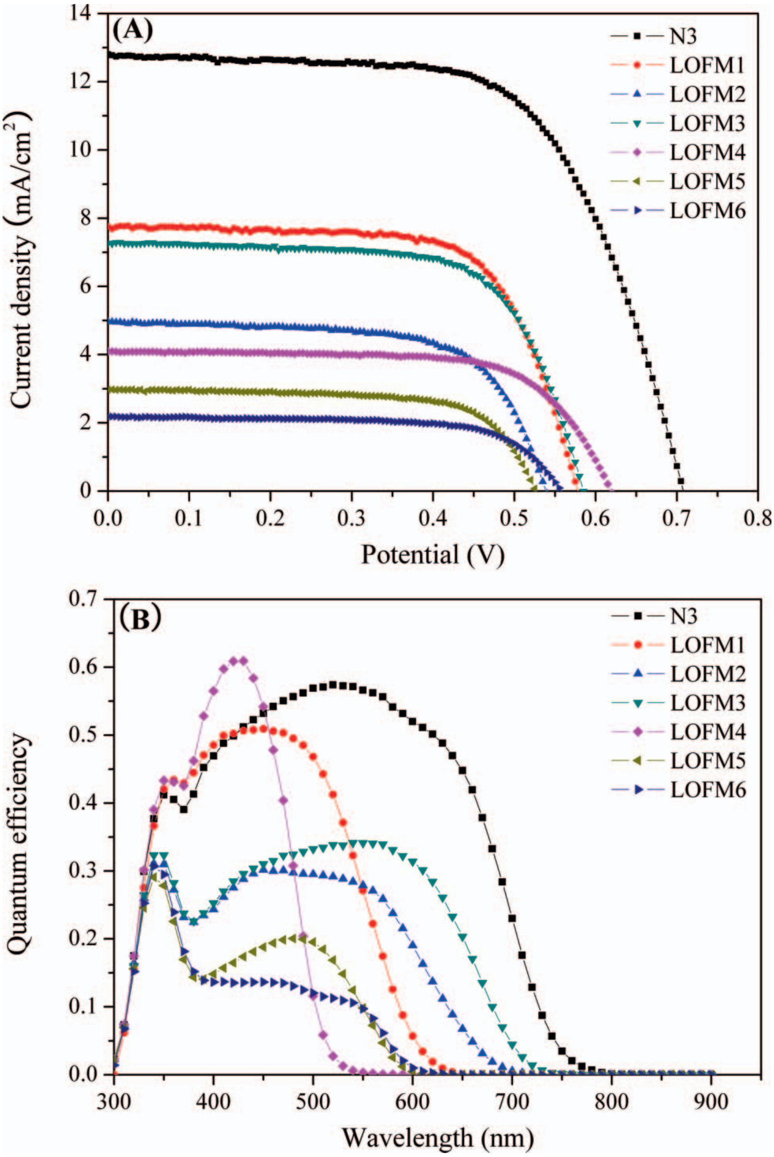

Figure 2. (A) Current density-voltage characteristics for DSSCs containing organic dyes under illumination of simulated solar light (AM 1.5, 100 mW/cm^2). (B) IPCE curves for DSSCs based on organic dyes. *Sample condition : Blocking layer, TiO_2 paste : B32, Organic Dye 0.5 mM – PMII(0.7 M) + LiI (0.2 M) + I_2 (0.05 M) + TBP (0.5 M) in ACN/VN = 85:15 - Pt electrode solution (7 mM), 60 μm surlyn, Dr. blade(2T).

flow depends on the photoelectric performance of the cell. Figure 3 shows the measured IS at forward bias applied condition under illumination. There are two well defined semicircles in high frequency region and middle frequency region. Compared with the results of LOFM4 ∼ LOFM6 dyes, the semicircle size in the middle frequency region of LOFM1 ∼

LOFM3 reduces significantly, indicating acceleration of electron transport process in the photoanode. The Bode-phases for DSSCs are also shown in Figure 3(B).

The frequency peaks of DSSC composed of LOFM4 ~ LOFM6 appeared in lower frequency region than those of DSSC with LOFM1 ~ LOFM3, due to relatively more rapid electron transfer process occurred in the LOFM1 ~ LOFM3. Since the frequency is related with the inverse of electron life time (τ) in TiO_2 electrodes, the higher electron life time were obtained in LOFM4 ~ LOFM6, compared to LOFM1 ~ LOFM3. Thus, in the case of LOFM1 ~ LOFM3, the lower electron life times reduce the V_{oc} values in the DSSC, as shown in Table 3. The performances of DSSCs containing respective N3 and organic dyes and the electron transport properties in their photoanodes from the IS analysis are summarized in Table 3.

Conclusions

The organic photo-sensitizers based on carbazole framework with multi-anchors/acceptors and thiophene bridge units were synthesized and applied to DSSCs. The multi-anchoring organic dyes with thiophene bridge provided efficient electron extraction pathways from electron donor, higher molar extinction coefficients, and better optical absorption in the longer

Table 2. Photovoltaic Performance of DSSCs. (Scattering layer; 250 nm, 4 μm + $TiCl_4$).

dyes	J_{sc} /mAcm^{-2}	V_{oc} /V	FF	η /%	Active area /cm^2	Layer thickn. /μm
N3	12.8	0.70	0.62	5.6	0.242	23.4
LOFM1	7.7	0.58	0.66	3.0	0.247	24.2
LOFM2	4.9	0.54	0.67	1.8	0.239	26.2
LOFM3	7.2	0.58	0.67	2.8	0.241	24.1
LOFM4	4.1	0.62	0.68	1.7	0.245	25.2
LOFM5	2.9	0.53	0.70	1.1	0.247	23.9
LOFM6	2.1	0.56	0.69	0.8	0.244	24.7

Table 3. Performances of the N3 and Organic dyes-based DSSCs and the electron transport properties in their photoanodes determined by impedance analysis. The cell areas are 0.24 cm^2.

dyes	R1(Ω)[a]	R2(Ω)[b]	C1[c]	R3(Ω)[d]	C2[e]	τ[f](ms)
N3	17.1	6.2	1.4×10^{-5}	18.7	1.2×10^{-3}	16.0
LOFM1	17.7	9.3	1.3×10^{-5}	18.2	2.6×10^{-4}	3.1
LOFM2	14.8	9.0	1.7×10^{-5}	33.1	8.1×10^{-5}	1.7
LOFM3	19.0	9.3	1.4×10^{-5}	21.0	2.8×10^{-4}	4.3
LOFM4	17.3	6.8	1.7×10^{-5}	49.0	7.6×10^{-4}	22.0
LOFM5	14.9	13.4	1.8×10^{-5}	50.3	8.4×10^{-5}	2.2
LOFM6	21.0	23.6	3.2×10^{-5}	82.2	3.5×10^{-4}	16.0

[a] R1 is FTO Interface resistance. [b] R2 is due to the resistance at the interface between the counter electrode and the electrolyte. [d] R3 is possibly originated from the backward charge transfer from TiO_2 to the electrolyte and the electron conduction in porous TiO_2 film.. [f] τ is life time of an electron in DSSC.

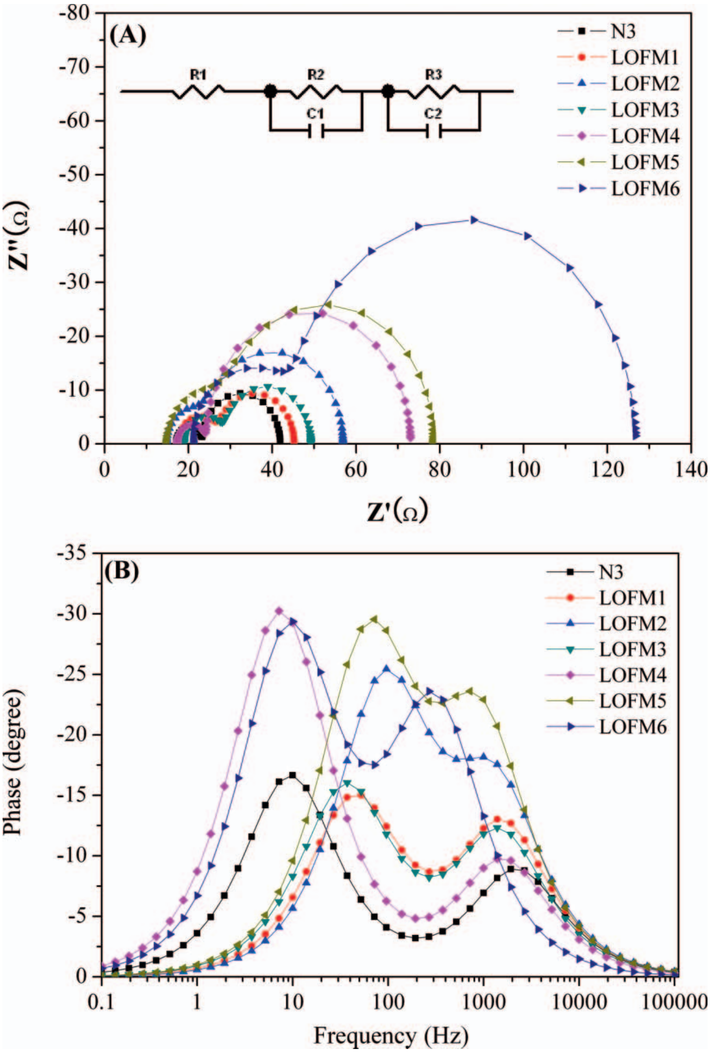

Figure 3. (A) Measured impedance spectra of DSSC at forward bias applied condition under light illumination. Fitted curve calculated using circuit shown in the inset. (B) Displays of Bode-phase for DSSC cell.

wavelengths, leading to improved short-circuit currents and overall energy-conversion efficiencies. We believe that practically useful organic dye photo-sensitizers can be produced by exploiting electron donor/acceptor system with proper length of π-conjugation in a chromophore to control the absorption wavelength and enhance the photovoltaic performance. The research on the spectral absorption optimization and the control of energy level of HOMO and LUMO for various organic dyes are now in progress.

Acknowledgment

This research was supported by the 2008 Yeungnam University Research Grant.

References

O'Regan, B., & Grätzel, M. (1991). *Nature*, **353**, 737.

Grätzel, M. (2001). *Nature*, **338**, 414.

Nazeeruddin, M. K., De Angelis, F., Fantacci, S., Selloni, A., Viscardi, G., Liska, P., Ito, S., Takeru, B., & Gratzel, M. (2005). *J. Am. Chem. Soc.*, **127**, 16835.

Baxter, J. B., & Aydil, E. S. (2005). *Appl. Phys. Lett.*, **86**, 053114.

Nazeeruddin, M. K., Kay, A., Rodicio, I., Humphry-Baker, R., Mueller, E., Liska, P., Valchopoulos, N., & Gratzel, M. (1993). *J. Am. Chem. Soc.*, **115**, 6382.

Nazeeruddin, M. K., Zakeeruddin, S. M., Humphry-Baker, R., Jirousek, M., Liska, P., Vlachopoulos, N., Shklover, V., Fischer, C.-H., & Gratzel, M. (1999). *Inorg. Chem.*, **38**, 6298.

Gratzel, M. (2005). *Inorg. Chem.*, **44**, 6841.

Horiuchi, T., Miura, H., Sumioka, K., & Uchida, S. (2004). *J. Am. Chem. Soc.*, **126**, 12218.

Wang, Z.-S., Cui, Y., Hara, K., Dan-oh, Y., Kasada, C., & Shinpo, A. (2007). *Adv. Mater.*, **19**, 1138.

Park, S. -S., Won, Y. -S., Choi, Y. -C., & Kim, J. -H. (2009). *Energy & Fuels*, **23**, 3732.

Tian, H., Yang, X., Cong, J., Chen, R., Liu, J., Hao, Y., Hagfeldt, A., & Sun, L. (2009). *Chem. Comm.*, 6288.

Hara, K., Sayama, K., Ohga, Y., Shinpo, A., Suga, S., & Arakawa, H. (2001). *Chem. Comm.*, 569.

Hagberg, D. P., Edvinsson, T., Marinado, T., Boschloo, G., Hagfeldt, A., & Sun, L. (2006). *Chem. Comm.*, 2245.

Thomas, K. R. J., Lin, J. T., Hsu, Y.-C., & Ho, K.-C. (2005). *Chem. Comm.*, 4098.

Velusamy, M., Thomas, K. R. J., Lin, J. T., Hsu, Y.-C., & Ho, K.-C. (2005). *Org. Lett.*, **7**, 1899.

Khazraji, A. C., Hotchandani, S., Das, S., & Kamat, P. V. (1997). *J. Phys. Chem. B.*, **103**, 4693.

William, F. M., Patti, E. B., John, C. R., Silvia, B. C., Lee, G. P., & David, G. W. (1984). *J. Am. Chem. Soc.*, **106**, 5659.